



2011-02-21

Radio-Frequency Breast Cancer Imaging Results for a Simplified Cylindrical Phantom

Giuseppe Ruvio

Technological University Dublin, Giuseppe.Ruvio@dit.ie

Raffaele Solimene

Seconda Università di Napoli, raffaele.solimene@unina2.it

Antonietta D'Alterio

Seconda Università di Napoli, antonietta.dalterio@unina2.it

Max Ammann

Dublin Institute of Technology, max.ammann@dit.ie

Rocco Pierri

Seconda Università di Napoli, rocco.pierri@unina2.it

Follow this and additional works at: <https://arrow.dit.ie/ahfrccon>

 Part of the [Bioimaging and Biomedical Optics Commons](#), and the [Biomedical Commons](#)

Recommended Citation

G. Ruvio, R. et al. (2011) Radio-frequency breast cancer imaging results for a simplified cylindrical phantom. *10th Int. Conference of the European Bioelectromagnetics Association, 2011, Rome*. ID 5250, ISBN 978-88-8286-231-2, doi:10.21427/D7K30H

This Conference Paper is brought to you for free and open access by the Antenna & High Frequency Research Centre at ARROW@TU Dublin. It has been accepted for inclusion in Conference Papers by an authorized administrator of ARROW@TU Dublin. For more information, please contact yvonne.desmond@dit.ie, arrow.admin@dit.ie, brian.widdis@dit.ie.



This work is licensed under a [Creative Commons Attribution-NonCommercial-Share Alike 3.0 License](#)



Radio-frequency breast cancer imaging results for a simplified cylindrical phantom

Giuseppe Ruvio^{1*}, Raffaele Solimene², Antonietta D'Alterio², Max J. Ammann¹ and Rocco Pierri²
¹Antenna & High Frequency Research Centre, Dublin Institute of Technology, Ireland
²Dipartimento di Ingegneria dell'Informazione, Seconda Università di Napoli, Italy,
^{*}giuseppe.ruvio@dit.ie

Introduction

As conventional X-ray mammography has been shown to be limited due to poor benign/malignant tissue contrast [1], the recent interest in active microwave based diagnostic approaches has proliferated. This technology takes advantage of a greater dielectric contrast between normal and diseased breast tissues in the UHF spectrum. RF breast cancer imaging technology can therefore have consequent high social and cost impact. Those important potential outcomes have triggered the investigation of many microwave imaging techniques, aiming at detecting, localizing and identifying cancers in breast tissues [2, 3].

Microwave imaging is a pervasive research field as it is proven to be useful in numerous applicative contexts where invasive inspections inside the object / scene under test are not possible. It also requires solving a very interesting and difficult mathematical problem since a non-linear and ill-posed problem must be tackled [4].

In this paper we perform a numerical investigation to assess the role played by fundamental parameters (i.e. number of sensors, operating frequency bandwidth) on cancer detection for a two-dimensional scenario. To this end, a simplified cylindrical phantom probed by ideal two-dimensional dipoles (i.e. infinitely long along the axis of invariance) is considered.

Models and Imaging algorithm

The cancer detection problem is treated by considering a coaxial cylindrical structure with a diameter $2r_s = 100\text{mm}$ which simulates the skin and breast tissue layers (see Fig. 1). As documented in [5], the tissues electromagnetic properties have been set as follows. The skin is modelled by using a conductivity σ_b of 4 S/m, a relative permittivity ϵ_{rb} of 36 and a thickness $r_s - r_b = 2\text{mm}$. The breast tissue is represented by using a first order Debye model with $\epsilon_s = 10$, $\epsilon_{\infty} = 7$, $\sigma = 0.15\text{ S/m}$ and relaxation time $\tau = 7.0\text{ ps}$. The tumour is a smaller cylinder of 5 mm diameter that is offset located with respect to the origin of the breast phantom. Its electromagnetic properties are given in terms of a Debye model with $\epsilon_{sc} = 54$, $\epsilon_{\infty c} = 4$, $\sigma_c = 0.7\text{ S/m}$ and $\tau_c = 7.0\text{ ps}$. Finally, the dielectric permittivity of the coupling medium ϵ_m is assumed equal to ϵ_s . The scattered field data are collected under a multimonostatic configuration (i.e. TX and RX are co-located) over a circle of radius $r_s = 55\text{mm}$ in correspondence to N measurement positions $(r_{o1}, r_{o2}, \dots, r_{oN})$.

As mentioned above, we are mainly interested in the detection and the localization of *small* tumours. Therefore, as only *qualitative* information is of concern (i.e. the degree of contrast of the scatterer is not asked to the imaging procedure), while developing the imaging algorithm, we conveniently adopt a linear model for the scattering phenomenon. Accordingly, said M the number of scatterers located at (r_1, r_2, \dots, r_M) , (with $N > M$), the scattered field vector can be written as

$$\underline{E}_S(f) = \underline{A}(f) \underline{b}(f) \quad (1)$$

where f is the frequency, \underline{b} is the $[M,1]$ vector of the in-homogeneities scattering coefficients and \underline{A} is $[N,M]$ propagator whose n -th column has the form $\underline{G}^n = [G^2(r_{o1}, r_n; f), G^2(r_{o2}, r_n; f), \dots, G^2(r_{oN}, r_n; f)]^T$, G being the relevant Green's function. Of course, the corresponding correlation matrix $\underline{R} = \underline{E}_S \underline{E}_S^H$ is rank deficient with rank one. However, \underline{G}^n evaluated in correspondence to points not coinciding with the scatterers' locations is orthogonal to the only significant singular vector $\underline{u}_1(f)$ of \underline{R} . This suggests to adopt the following scheme to identify the scatterers' locations

$$P(r_i) = \frac{1}{|\log (| \langle \underline{G}^i(f_1), \underline{u}_1(f_1) \rangle \cdot \langle \underline{G}^i(f_2), \underline{u}_1(f_2) \rangle |) |} \quad (2)$$

where \underline{G}^i is evaluated at the trial position r_i and $\langle \cdot, \cdot \rangle$ denotes the Hermitian scalar product. Accordingly, detection is

achieved for non-zero values of P . Note that in eq. (2), we have considered the “beating” between the projections at two different frequencies. This helps in reducing the occurrence of spurious artefacts and, in general, more than two frequencies can be considered. We expect that this procedure succeeds at least for a limited number of in-homogeneities.

Numerical results

In this section, the algorithm is checked in the presence of one in-homogeneity against the noise and for different working frequencies. To this end, an FDTD based numerical tool is used to solve the forward scattering problem. Subsequently, the time-domain data are Fourier transformed to make them suitable for eq. (2). In particular, the scattered field is collected over 12 different positions taken uniformly $(360/12)^\circ$ whereas the tumour’s centre is at $(25,25)$ mm. In Fig. 1 two reconstruction examples are reported. Fig. 1b refers to single frequency data at $f=1$ GHz, whereas Fig. 1c two frequencies, $f_1=1$ GHz and $f_2=2.5$ GHz, are exploited. In both cases the tumour is well detected. However, in the single-frequency case the tumour appears slightly delocalized at $(27,27)$ mm. The algorithm has been also tested for data corrupted by an additive zero mean complex Gaussian noise. Detection is resilient up to Signal-to-Noise ratio figure of 10dB.

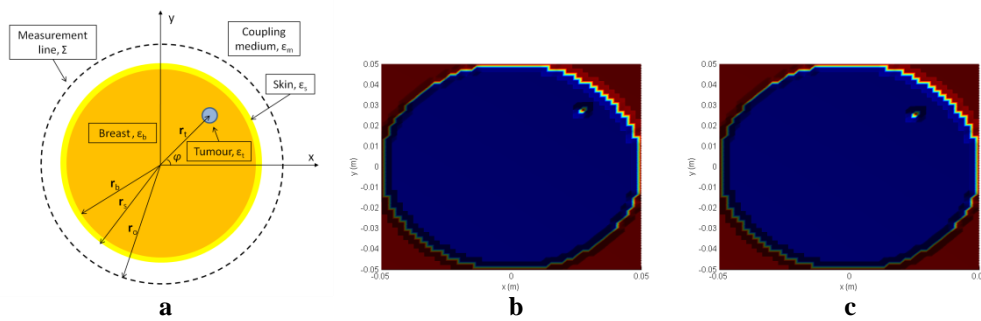


Figure 1: **a:** Configuration layout; **b:** Reconstruction obtained at single frequency; **c:** Reconstruction obtained by exploiting two frequencies.

Conclusions

Aside the mathematical problem that is relevant for imaging algorithm/method development, some crucial questions must be addressed in practical scenarios. Among them, the transmitting antenna behaviour must be estimated / compensated. Otherwise, as antennas shape the transmitted signal spectrum and introduce phase variation, blurred and delocalized reconstructions are obtained. To solve this problem, in principle, the antennas behaviour can be compensated by a preliminary calibration step or estimated (by numerical experiments or measurements) so that it can be enclosed in the mathematical formulation of the problem and, hence, be properly exploited in the imaging algorithm. In particular, while pursuing such a task, one must care that antennas are in close proximity to the breast. While the algorithm detection capability has been tested for an ideal dipole source, results concerning a realistic antenna will be addressed at the conference.

References

- [1] P. T. Huynh, A. M. Jorolimek, and S. Dave, “The False-negative mammogram,” *Radiograph*, vol. 18, no. 5, pp. 1137-1154, 1998.
- [2] E. J. Bond, X. Li, S. C. Hagness, and B. D. V. Veen, “Microwave imaging via space-time beamforming for early detection of breast cancer,” *IEEE Trans. Antennas Propag.*, vol. 51, pp. 1690–1705, 2003.
- [3] S. M. Salvador, and G. Vecchi, “Experimental tests of microwave breast cancer detection on phantoms,” *IEEE Trans. Antennas Propag.*, vol. 57, no. 6, pp. 1705-1712, June 2009.
- [4] Z. Q. Zhang, and Q. H. Liu, “Three-dimensional nonlinear image reconstruction for microwave biomedical imaging,” *IEEE Trans. Biomed. Eng.*, vol. 51, pp. 544–548, Mar. 2004.
- [5] Y. Chen, E. Gunawan, K. S. Low, S.-C. Wang, C. B. Soh, and T. C. Putti, “Time-Reversal Ultrawideband Breast Imaging: Pulse Design Criteria Considering Multiple Tumors With Unknown Tissue Properties,” *IEEE Trans. Antennas Propag.*, vol. 56, no. 9, pp. 3073-3077, Sept. 2008.